

## Factors Governing the Kinetic Competition of Nitrogen and Sulfur Ligands in Cisplatin Binding to Biological Targets<sup>†</sup>

Dirk V. Deubel\*

Contribution from the Department of Chemistry and Applied Biosciences, ETH Zürich, Computational Science Laboratory, USI Campus, 6900 Lugano, Switzerland

Received January 3, 2004; E-mail: metals-in-medicine@phys.chem.ethz.ch

**Abstract:** The kinetic competition of sulfur and nitrogen nucleophiles L in the substitution reactions of cisplatin derivatives,  $cis-[Pt^{II}(NH_3)_2(X)(OH_2)]^{n+} + L \rightarrow cis-[Pt^{II}(NH_3)_2(X)(L)]^{m+} + H_2O$  ( $X = Cl^-, H_2O$ ), has been studied using density functional theory and continuum dielectric calculations. The calculations reveal an intrinsic kinetic preference of platinum(II) for nitrogen over sulfur ligands. However, biologically relevant substituents can mask this preference for nitrogen nucleophiles. Investigation of the activation free energies of the substitution reactions in dependence of the dielectric constant  $\epsilon$  demonstrates the microenvironment to be crucial in the binding of cisplatin to its intracellular targets. The fused aromatic heterocycle of guanine stabilizes the transition state for platination at a smaller  $\epsilon$  more efficiently than do the functional groups of amino acid residues. The results of this work suggest a relatively facile platination of guanine-N7 sites of DNA in regions of low  $\epsilon$ , particularly in the proximity of histone cores.

### Introduction

A central theme in the discussion of the mode of action of the anticancer drug cisplatin ( $cis-[Pt(NH_3)_2Cl_2]$ )<sup>1</sup> have been the questions why and how cisplatin reaches its ultimate target, the N7 sites of the DNA purine bases. Because of the strong affinity of the soft metal to sulfur-donor ligands, “one would predict that platinum(II) compounds would perhaps never reach the DNA, with many platinumophiles such as glutathione or methionine as competing ligands in the cytosol”.<sup>2</sup> Experimental competition studies in aqueous solution indicated that the reaction of model complexes such as  $\{Pt(dien)\}^{2+}$  derivatives with thioethers is often kinetically favored to that with guanines, leading to a current opinion that platinum anticancer drugs kinetically prefer sulfur over nitrogen donors.<sup>3</sup> Herein I wish to present a combined density functional theory (DFT) and continuum dielectric model (CDM) study<sup>4</sup> aiming to elucidate the kinetic competition of nitrogen and sulfur ligands in their reactions with  $cis$ -diammineaquachloroplatinum(II) ( $cis-[Pt(NH_3)_2(OH_2)Cl]^+$ ,

**1**) and  $cis$ -diamminediaquaplatinum(II), ( $cis-[Pt(NH_3)_2(OH_2)_2]^{2+}$ , **2**). **1** and **2** are active species generated by partial hydrolysis of the drug in the cell (Figure 1).<sup>1,5</sup> While this work was in preparation, Baik et al.<sup>8</sup> reported a complementary DFT study on the reaction of cisplatin derivatives with adenine and guanine to explain why adenine platination is less favored.

In this work, I predict and rationalize the activation barriers of the reactions of **1** and **2** with nitrogen and sulfur nucleophiles L,  $[Pt^{II}(NH_3)_2(X)(OH_2)]^{n+} + L \rightarrow cis-[Pt^{II}(NH_3)_2(X)(L)]^{m+} + H_2O$  ( $X = Cl^-, H_2O$ ), in various ways. In part 1, The Heteroatom, I compare the reactions of the cisplatin derivatives **1** and **2** with two simple nucleophiles containing N and S heteroatoms,  $NH_3$  and  $H_2S$ . In particular, an energy decomposition analysis along the reaction paths is performed to reveal the factors that determine the activation energies. In part 2, The Substituents, the influence of biologically relevant substituents on the activation barriers has been studied. In part 3, The

<sup>†</sup> Quantum Chemical Studies of Metals in Biology and Medicine, III. Part II: ref 29d.

(1) (a) *Cisplatin*; Lippert, B., Ed.; Wiley-VCH: Weinheim, Germany, 1999. (b) Wong, E.; Giandomenico, C. M. *Chem. Rev.* **1999**, *99*, 2451. (c) Jamieson, E. R.; Lippard, S. J. *Chem. Rev.* **1999**, *99*, 2467. (d) Guo, Z. J.; Sadler, P. J. *Angew. Chem., Int. Ed.* **1999**, *38*, 1513. (e) *Platinum-Based Drugs in Cancer Therapy*; Kelland, L. R., Farrell, N., Eds.; Humana Press: Totowa, NJ, 2000. (f) Hambley, T. W.; Jones, A. R. *Coord. Chem. Rev.* **2001**, *212*, 35. (g) Fuertes, M. A.; Alonso, C.; Perez, J. M. *Chem. Rev.* **2003**, *103*, 645. (h) Zhang, C. X.; Lippard, S. J. *Curr. Opin. Chem. Biol.* **2003**, *7*, 481.

(2) Reedijk, J. *Proc. Natl. Acad. Sci. U.S.A.* **2003**, *100*, 3611.

(3) Selected examples: (a) Reedijk, J. *Chem. Rev.* **1999**, *99*, 2499 and references cited therein. (b) Murdock, P. D.; Kratchowil, N. A.; Parkinson, J. A.; Patriarca, M.; Sadler, P. J. *Angew. Chem., Int. Ed.* **1999**, *38*, 2949. (c) Teuben, J.-M.; Reedijk, J. *J. Biol. Inorg. Chem.* **2000**, *5*, 463. (d) Marchan, V.; Moreno, V.; Pedroso, E.; Grandas, A. *Chem.-Eur. J.* **2001**, *7*, 808. (e) Hahn, M.; Kleine, M.; Sheldrick, W. S. *J. Biol. Inorg. Chem.* **2001**, *6*, 556. (f) Fakih, S.; Munk, V. P.; Shipman, M. A.; Murdock, P. D.; Parkinson, J. A.; Sadler, P. J. *Eur. J. Inorg. Chem.* **2003**, 1206.

(4) Selected quantum chemical studies of cisplatin: (a) Zhang, Y.; Guo, Z. J.; You, X. Z. *J. Am. Chem. Soc.* **2001**, *123*, 9378. (b) Baik, M. H.; Friesner, R. A.; Lippard, S. J. *J. Am. Chem. Soc.* **2002**, *124*, 4495. (c) Deubel, D. V. *J. Am. Chem. Soc.* **2002**, *124*, 5834. (d) Burda, J. V.; Sponer, J.; Hrabadkova, J.; Zeizinger, M.; Leszczynski, J. *J. Phys. Chem. B* **2003**, *107*, 5349. (e) Burda, J. V.; Leszczynski, J. *Inorg. Chem.* **2003**, *42*, 7162. (f) Baik, M. H.; Friesner, R. A.; Lippard, S. J. *Inorg. Chem.* **2003**, *42*, 8615. (g) Costa, L. A. S.; Rocha, W. R.; De Almeida, W. B.; Dos Santos, H. F. *J. Chem. Phys.* **2003**, *118*, 10584. (h) Chval, Z.; Sip, M. *Collect. Czech. Chem.* **2003**, *C68*, 1105. (i) Burda, J. V.; Zeizinger, M.; Leszczynski, J. *J. Chem. Phys.* **2004**, *120*, 1253.

(5) The two compounds **1** and **2** considered herein and in other computational studies (refs 8 and 11) represent monocationic and dicationic cisplatin hydrolysis products. Hydroxo species may be formed upon deprotonation, and their reactivity to biomolecules is anticipated to be similar to that of the chloro analogues. The experimental  $pK_a$  of **1** is 6.41 and the  $pK_a$ 's of **2** are 5.37 and 7.21 (ref 6). Note that the pH close to the surface of DNA may be significantly lower than that of bulk solution (ref 7).

(6) Berners-Price, S. J.; Frenkiel, T. A.; Frey, U.; Ranford, J. D.; Sadler, P. J. *Chem. Commun.* **1992**, 789.

(7) Lamm, G.; Pack, G. R. *Proc. Natl. Acad. Sci. U.S.A.* **1990**, *87*, 9033.

(8) Baik, M. H.; Friesner, R. A.; Lippard, S. J. *J. Am. Chem. Soc.* **2003**, *125*, 14082.

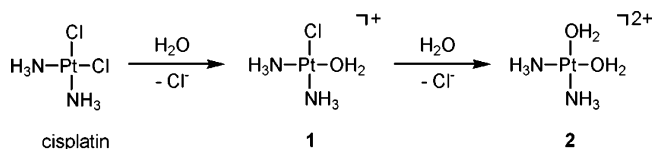


**Figure 1.** Activation of the anticancer drug cisplatin by hydrolysis.

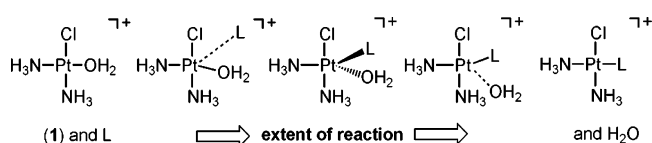


**Figure 2.** Substitution of the aqua ligand in *cis*-[Pt(NH<sub>3</sub>)<sub>2</sub>(OH<sub>2</sub>)Cl]<sup>+</sup> (**1**) with nucleophile L.

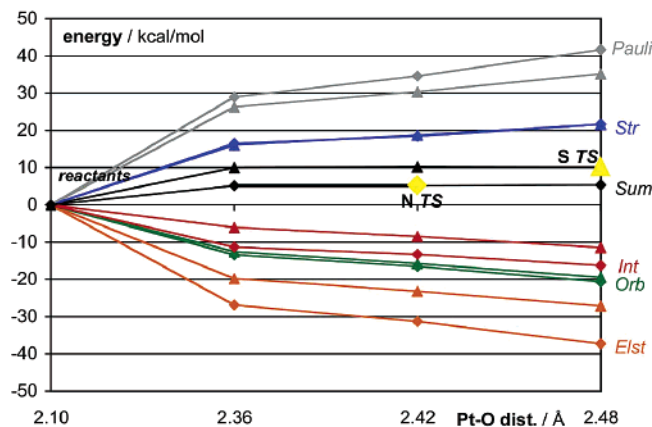


**Figure 3.** Energy decomposition in the reaction of **1** with ammonia (N, rhombuses) and hydrogen sulfide (S, triangles).

Environment, environmental effects by continuum dielectric calculations have been investigated to consider the fact that a large fraction of the cell consists of compounds other than water. These regions of the cell may be characterized by a dielectric constant  $\epsilon$  that is significantly lower than that of water. This consideration has serious consequences for the relative reactivity of cisplatin derivatives to various biomolecules.

## Results and Discussion

**1. The Heteroatom.** To verify and rationalize the kinetic preference of platinum(II) complexes for sulfur ligands, I have investigated the interaction of *cis*-[Pt(NH<sub>3</sub>)<sub>2</sub>(OH<sub>2</sub>)Cl]<sup>+</sup> (**1**) with L = NH<sub>3</sub> and H<sub>2</sub>S during the nucleophilic substitution reaction,  $\mathbf{1} + \text{L} \rightarrow \text{cis-}[\text{Pt}(\text{NH}_3)_2(\text{L})\text{Cl}]^+ + \text{H}_2\text{O}$ , using the Ziegler–Rauk energy decomposition scheme.<sup>9</sup> If this scheme is directly employed for analyzing transition states (TS), the distance dependence of the energy contributions may result in misleading conclusions, because the transition state for the reaction of **1** with NH<sub>3</sub> occurs at a smaller extent of reaction (see Figure 2) than that with H<sub>2</sub>S, as indicated by Pt–O distances of 2.42 and 2.48 Å in the TS. Therefore, a series of points along the reaction coordinate has been considered by adding to the TS geometry a fraction of the Hessian eigenvector that corresponds to the imaginary frequency. The results of the analysis are displayed in Figure 3.

Surprisingly, the reaction of **1** with NH<sub>3</sub> has a 5 kcal/mol lower activation energy than that with H<sub>2</sub>S, demonstrating an

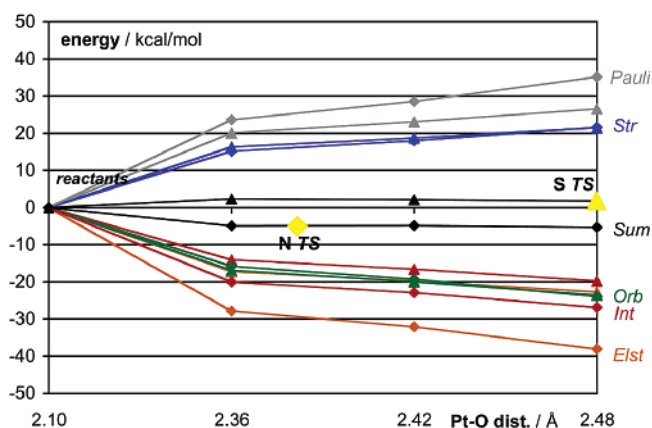


**Figure 4.** Energy decomposition in the reaction of **2** with ammonia (N, rhombuses) and hydrogen sulfide (S, triangles).

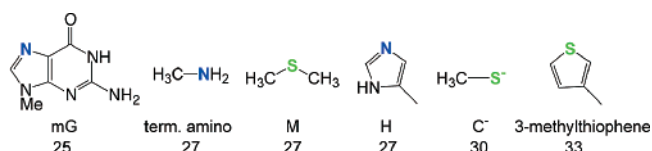


**Figure 5.** Calculated activation free energies  $\Delta G_a$  (in kcal/mol) for the reaction  $\mathbf{1} + \text{L} \rightarrow \text{cis-}[\text{Pt}(\text{NH}_3)_2\text{Cl}(\text{L})]^{m+} + \text{H}_2\text{O}$ , in water ( $\epsilon = 80$ ).

intrinsic kinetic preference of **1** for nitrogen ligands. According to the analysis in Figure 1, both reactions require a similar deformation of the reactant **1** toward the TS geometry, as indicated by a similar strain energy (*Str*, blue). The amount of stabilizing orbital interactions (*Orb*, green) between the reactants is also similar in both reactions. However, electrostatic interactions (*Elst*, orange) stabilize the reaction of NH<sub>3</sub> more strongly than that of H<sub>2</sub>S. This difference is only partly offset by a slightly stronger Pauli repulsion (*Pauli*, gray) between **1** and NH<sub>3</sub>. Hence, the interaction energy ( $\text{Int} = \text{Pauli} + \text{Elst} + \text{Orb}$ , red) is more negative upon nucleophilic attack of NH<sub>3</sub>, resulting in a smaller (less positive) sum of the barrier-determining energies in the reaction of NH<sub>3</sub> ( $\text{Sum} = \text{Str} + \text{Int}$ , black). The activation energy corresponds to *Sum* at the TS (yellow).

Figure 4 displays the results of the analysis of the reaction of the dicationic species *cis*-[Pt(NH<sub>3</sub>)<sub>2</sub>(H<sub>2</sub>O)<sub>2</sub>]<sup>2+</sup> (**2**) with NH<sub>3</sub> and H<sub>2</sub>S. In comparison with the reaction of **1**, Pauli repulsion is reduced and the stabilizing electrostatic and orbital interactions are slightly stronger in the reactions of **2**. This leads to the effect that in vacuo the energy of the transition state for the reaction of **2** with ammonia is smaller than that of the isolated reactants, which will be compensated by the greater stabilization of the dicationic complexes in solution (vide infra). The differences between the energy components in the reactions of **2** to the N and S nucleophiles are similar to those in the reactions of **1**. The dicationic species *cis*-[Pt(NH<sub>3</sub>)<sub>2</sub>(H<sub>2</sub>O)<sub>2</sub>]<sup>2+</sup> (**2**) shows a slightly larger kinetic preference ( $\sim 7$  kcal/mol) for nitrogen over sulfur ligands than does the monocationic species **1** ( $\sim 5$  kcal/mol).

**2. The Substituents.** To investigate the effect of biologically relevant substituents at the nitrogen and sulfur ligands on the reactivity of **1** in aqueous solution, I have calculated the activation free energies  $\Delta G_a$  for the reaction of **1** with various nucleophiles using DFT and a CDM with a dielectric constant  $\epsilon = 80$  for water (Figure 5). This approach predicts similar activation free energies for the reaction of **1** with dimethyl

(9) Bickelhaupt, F. M.; Baerends, E. J. In *Reviews in Computational Chemistry*; Lipkowitz, K. B., Boyd, D. B., Eds.; VCH: New York, 2000; Vol. 15, p 1.

sulfide (M, representing methionine) and 5-methylimidazole (H, representing histidine). However, **1** is predicted to be significantly more reactive to H than to 3-methylthiophene (Figure 5). Note that the latter molecule has no biological relevance but serves here as a sulfur-analogue of 3-methylimidazole. The calculations indicate that nitrogen ligands are, in general, preferred to sulfur ligands, if the substituents at the heteroatoms are similar. Although aminomethane (representing deprotonated terminal amino groups,  $pK_a = 8.0$ )<sup>10</sup> contains only one electron-donating methyl substituent, it is predicted to be as reactive to **1** as is dimethyl sulfide (Figure 5). The activation free energy for methanethiolate ( $C^-$ , representing the amount of glutathione and cysteine ( $pK_a = 8.3$ )<sup>10</sup> that is deprotonated) is predicted to be higher than that of M, which is attributed to the stabilization of the  $C^-$  anion in aqueous solution. The TS for the reaction of the cisplatin derivative with mG is stabilized by hydrogen bonding, as analyzed in detail in ref 8.

The results of this section demonstrate that the superficial classification, “nitrogen versus sulfur ligands”, is no longer warranted in the discussion of the mode of action of platinum anticancer drugs. Substituents at the heteroatom may influence the reactivity of nucleophiles to the metal complex in the same order of magnitude as does the heteroatom itself. The stereo-electronic characteristics of the nucleophile, i.e., the presence of aliphatic substituents or the integration in an aromatic heterocycle, can mask the intrinsic kinetic preference of platinum(II) for nitrogen ligands.

**3. The Environment.** To consider the fact that approximately 30 wt % of the cell consists of compounds other than water, I have systematically investigated the activation free energies in dependence of the dielectric constant  $\epsilon$ .  $\epsilon$  of DNA in water was estimated to be 24,<sup>11</sup> whereas  $\epsilon$  of proteins is typically estimated to be lower than 10 and might be as low as 3, depending on whether the site of interest is located on the protein surface, solvent-exposed, or deeply buried in the protein interior.<sup>12</sup>

Figures 6 and 7 emphasize the trends in the predicted reaction and activation free energies,  $\Delta G_r$  and  $\Delta G_a$ , for the reaction of **1** and **2** with 9-methylguanine (mG), 5-methylimidazole (H), dimethyl sulfide (M), and methanethiolate ( $C^-$ ) at  $\epsilon = 3, 9, 24$ , and 80.<sup>13</sup> Comparing the reaction of **1** and **2** with H and mG shows H to be (i) thermodynamically more favored than mG at  $\epsilon \geq 9$ , but (ii) kinetically less favored than mG at each  $\epsilon$ . Comparing the reaction of **1** and **2** with M and mG indicates that M is kinetically and thermodynamically less favored, in particular, (i) at relatively small  $\epsilon$  and (ii) in the reaction of **2**. The results for the reactions of  $C^-$  predict the trend that, at large  $\epsilon$ ,  $C^-$  is thermodynamically rather than kinetically competitive to mG.<sup>14</sup> Comparing the reaction of **1** and **2** with

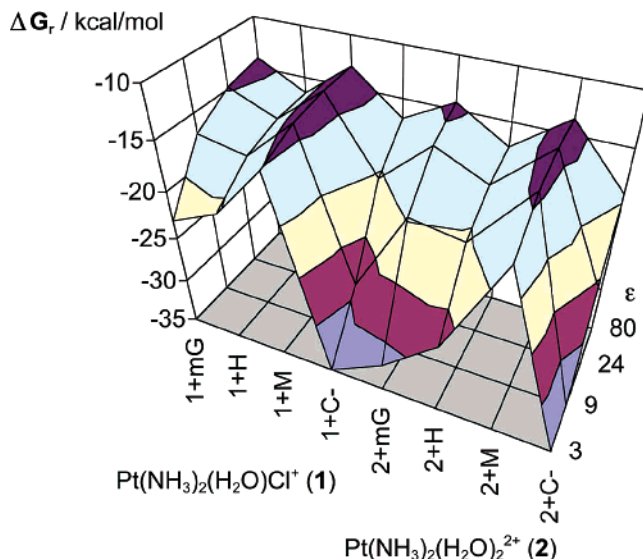


**Figure 6.** Calculated reaction free energies  $\Delta G_r$  (in kcal/mol) for the reactions **1** + L  $\rightarrow$  *cis*-[Pt(NH<sub>3</sub>)<sub>2</sub>Cl(L)]<sup>m+</sup> + H<sub>2</sub>O and **2** + L  $\rightarrow$  *cis*-[Pt(NH<sub>3</sub>)<sub>2</sub>(H<sub>2</sub>O)(L)]<sup>n+</sup> + H<sub>2</sub>O at various  $\epsilon$ . L = 9-methylguanine (mG), 5-methylimidazole (H), dimethyl sulfide (M), and methanethiolate ( $C^-$ ).

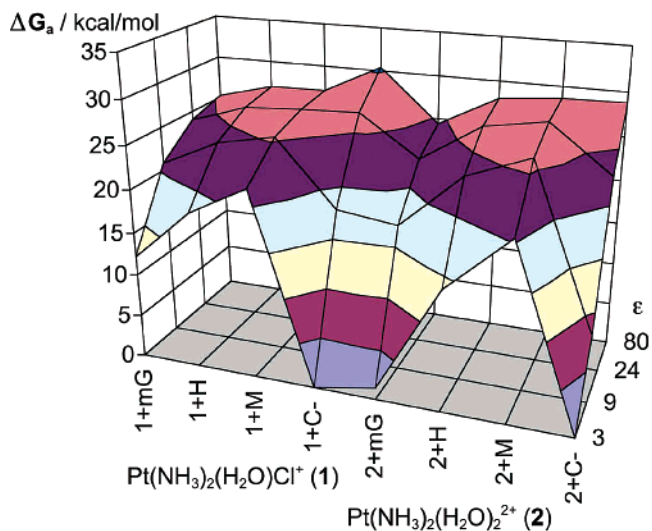


**Figure 7.** Calculated activation free energies  $\Delta G_a$  (in kcal/mol) for the reactions **1** + L  $\rightarrow$  *cis*-[Pt(NH<sub>3</sub>)<sub>2</sub>Cl(L)]<sup>m+</sup> + H<sub>2</sub>O and **2** + L  $\rightarrow$  *cis*-[Pt(NH<sub>3</sub>)<sub>2</sub>(H<sub>2</sub>O)(L)]<sup>n+</sup> + H<sub>2</sub>O at various  $\epsilon$ .

mG indicates the activation free energy for the reaction of **2** to be lower than that of **1**. The reaction of **2** with mG is specifically stabilized by an O—H $\cdots$ O hydrogen bond from the *cis*-aqua ligand of **2** to mG—O.<sup>6</sup> The corresponding TS with an N—H $\cdots$ O<sup>6</sup> hydrogen bond involving an ammine ligand of **2** rather than the aqua ligand is calculated to be 4 kcal/mol higher in energy (cf. ref 8).

The largest differences in the activation free energies of the reactions of *cis*-[Pt(NH<sub>3</sub>)<sub>2</sub>(OH<sub>2</sub>)Cl]<sup>+</sup> (**1**) with various nucleophiles are observed at low  $\epsilon$ , with  $\Delta G_a$  increasing in the order:  $C^- < mG < H < M$  (Figure 7).  $C^-$  is the only anionic nucleophile considered, and its approach to the cationic complex **1** is strongly stabilized. In contrast, M is a neutral alkyl-substituted sulfur nucleophile. H is an aromatic heterocycle, while mG is a fused aromatic heterocycle that includes a hydrogen bond acceptor at O<sup>6</sup>. The aromatic heterocycles H and especially mG partly mimic the effect of the polarizable

- (10) Berg, J. M.; Tymoczko, J. L.; Stryer, L. *Biochemistry*, 5th ed.; W. H. Freeman: New York, 2002.
- (11) Monjardet-Bas, V.; Elizondo-Riojas, M. A.; Chottard, J. C.; Kozelka, J. *Angew. Chem., Int. Ed.* **2002**, *41*, 2998.
- (12) Archontis, G.; Simonson, T. *J. Am. Chem. Soc.* **2001**, *123*, 11047 and references cited therein.
- (13) Figure 6 displays  $\Delta G_r$  values smaller than  $-35$  kcal/mol as  $-35$  kcal/mol; Figure 7 displays  $\Delta G_a$  values smaller than 0 as 0 kcal/mol. For data tables, see Supporting Information.
- (14) The  $\Delta G_a$  values for the reactions with  $C^-$  at low  $\epsilon$  would be very small (or appear to be negative due to the formation of an adduct with the Pt(II) complex in a vacuum, cf. refs 4a and 8), but the consideration of thiolates at low  $\epsilon$  is biologically not relevant because the  $pK_a$  of thiols strongly increases with decreasing  $\epsilon$  (see Supporting Information, Table S-6). The free-energy profiles for thiols are anticipated to be similar to those for thioethers. Thiols may first react with the Pt(II) complex and become deprotonated subsequently.



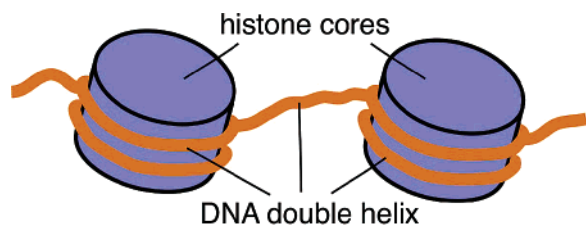


**Figure 8.** Schematic representation of the wrapping of DNA around the histone cores of nucleosomes.

environment at low  $\epsilon$ .<sup>15</sup> The differences in  $\Delta G_a$  are compensated by a larger dielectric constant, because the solvation of small charged platinum complexes is more efficient than that of the larger complexes. The activation free energies of the reactions of the dicationic species  $cis\text{-}[\text{Pt}(\text{NH}_3)_2(\text{OH}_2)_2]^{2+}$  (**2**) show the same trends at low  $\epsilon$  as those of the monocationic species **1** but to a greater extent. On the other hand, the differences in  $\Delta G_a$  at high  $\epsilon$  are not very large, because the dicationic complexes are more efficiently solvated than the monocationic species. As mentioned before, the thermodynamics of the reactions show some subtle deviations from the kinetics. For a given reaction with one of the neutral nucleophiles, the calculated trends are very similar at each  $\epsilon$ , indicating that the deviations arise mainly from the intrinsic stabilization of the transition states and products rather than from solvation effects. For instance, at  $\epsilon = 3$ ,  $\Delta G_a$  for the reaction of **1** with mG is 6 kcal/mol lower than that of the reaction of **1** with H, while the mG product is only 2 kcal/mol more stable than the H product. At  $\epsilon = 80$ , the mG TS is more stable than the H TS by 2 kcal/mol, while the mG product is 2 kcal/mol less stable than the H product.

The stabilization of the transition states for mG platination at low  $\epsilon$  relative to the TS for the platination of neutral amino acid residues is one of the most important findings of this work. This result is particularly relevant to the tight wrapping of DNA around the histone heterooctamers of nucleosomes (Figure 8),<sup>16</sup> which likely provide a microenvironment of a considerably lower dielectric constant than that of DNA in aqueous solution. Recall that histones are present in such a tremendous quantity in a eukaryotic cell that their total mass equals that of the DNA.<sup>17</sup> The high reactivity of guanine sites to cisplatin derivatives in the vicinity of DNA–protein complexes could not be discovered in experimental competition studies in aqueous solution.<sup>3</sup> The quaternary structure of DNA in the cell nucleus promotes cisplatin binding to its ultimate target.

The presence of the low  $\epsilon$  regions in the chromatin likely has far-reaching consequences for the reactions of other metal complexes with nuclear DNA. One example is the binding of titanium(IV) anticancer complexes to phosphodiester. Guo et al.<sup>18</sup> observed that titanocene dichloride does not react with 3',5'-cyclic GMP in aqueous solution. However,  $\text{Cp}_2\text{TiCl}_2$  does react with cGMP and with the dinucleotide GpC in the less polar

solvent dimethyl formamide.<sup>18</sup> The dielectric properties of the medium may induce a chemoselectivity of metal binding that differs from what would have been anticipated from the chemistry of the metal complexes in aqueous solution. The reactions of nonplatinum metallopharmaceuticals with potential biological targets in different environments are presently under investigation in our Computational Science Laboratory.

## Conclusions

The activation free energies for the reaction of the cisplatin derivatives  $cis\text{-}[\text{Pt}(\text{NH}_3)_2(\text{OH}_2)\text{Cl}]^+$  (**1**) and  $cis\text{-}[\text{Pt}(\text{NH}_3)_2(\text{OH}_2)_2]^{2+}$  (**2**) with nitrogen and sulfur-containing amino acid residues and 9-methylguanine depend on three factors in the following manner:

1. The Heteroatom. Contrary to common belief, platinum-(II) complexes show an intrinsic kinetic preference for nitrogen over sulfur nucleophiles, as indicated by comparing the reactions of **1** and **2** with ammonia and dihydrogensulfide. An analysis of the components that determine the activation energies shows the preference for the nitrogen ligand to arise from electrostatic interactions along the reaction coordinate rather than from stabilizing orbital interactions.

2. The Substituents. The influence of biologically relevant substituents, i.e., the presence of alkyl groups or an aromatic heterocycle, on the activation free energies can be as strong as the effect of the heteroatom itself. For instance, the calculations predict similar activation free energies in aqueous solution ( $\epsilon = 80$ ) for the reaction of **1** with dimethyl sulfide (representing methionine) and 5-methylimidazole (representing histidine), but much larger activation free energy for the reaction of **1** with 3-methylthiophene, a sulfur-analogue of 5-methylimidazole.

3. The Environment. Investigation of the activation free energies in dependence of the dielectric constant  $\epsilon$  shows the environment to be crucial in the reactivity and selectivity in the reactions of metal complexes with biomolecules. The fused aromatic heterocycle of guanine stabilizes the transition state for platination at a smaller  $\epsilon$  more efficiently than do the functional groups of amino acid residues. DNA–nucleosome complexes likely provide a microenvironment with a lower dielectric constant than that of DNA in aqueous solution, thus promoting cisplatin binding to the N7 sites of guanine.

## Computational Methods

**Structures and Energies.** The geometries of molecules and transition states (TS) were optimized at the gradient-corrected DFT level using the 3-parameter fit of exchange and correlation functionals of Becke (B3LYP),<sup>19</sup> which consists of a linear combination of the exchange functionals of Dirac,<sup>20</sup> Fock,<sup>21</sup> and Becke<sup>22</sup> and of the correlation functionals of Vosko, Wilk, and Nusair<sup>23</sup> and of Lee, Yang, and Parr (LYP),<sup>24</sup> as implemented in Gaussian 98.<sup>25</sup> The shape-consistent scalar-relativistic small-core ECP of Hay and Wadt<sup>26</sup> and the corresponding basis set were used at platinum (LANL2DZ). 6-31G(d) all-electron basis sets were used at the other atoms,<sup>27</sup> while the basis set on the hydrogen atoms of the ammine or aqua ligand involved in hydrogen bonding to guanine-O<sup>6</sup> included additional polarization functions (6-31G(d,p)). This basis set combination is denoted II–. Vibrational frequencies were also calculated at B3LYP/II–. The

(15) Test calculations indicate that the stabilization of the TS and product of the reaction of **1** with 3-methylimidazole at low  $\epsilon$  is attributed to the electronic structure rather than to the larger size of the nucleophile: At  $\epsilon = 1$  and 80, the predicted  $\Delta G_a$ 's for the reaction of **1** with 1-aminopentane are very similar to those of aminomethane rather than to those of 3-methylimidazole.

(16) Luger, K.; Mäder, A. W.; Richmond, R. K.; Sargent, D. F.; Richmond, T. J. *Nature* **1997**, *389*, 251.

(17) Alberts, B.; Johnson, A.; Lewis, J.; Raff, M.; Roberts, K.; Walter P. *Molecular Biology of the Cell*; Garland: New York, 4th ed., 2002.

(18) Guo, M. L.; Guo, Z. J.; Sadler, P. J. *J. Biol. Inorg. Chem.* **2001**, *6*, 698.

(19) Becke, A. D. *J. Chem. Phys.* **1993**, *98*, 5648.

(20) Dirac, P. A. M. *Proc. Camb. Philos. Soc.* **1930**, *26*, 376.

(21) Fock, V. *Z. Physik* **1930**, *61*, 161.

(22) Becke, A. D. *Phys. Rev. A* **1988**, *38*, 3098.

(23) Vosko, S. H.; Wilk, L.; Nusair, M. *Can. J. Phys.* **1980**, *58*, 1200.

(24) Lee, C. T.; Yang, W. T.; Parr, R. G. *Phys. Rev. B* **1988**, *37*, 785.

structures reported are either minima (NIMAG = 0) or transition states (NIMAG = 1) on the potential energy surfaces. Improved total energies were calculated at the B3LYP level using the same ECP and valence basis set at the metal, but totally uncontracted and augmented with Frenking's set of f functions,<sup>28</sup> together with the 6-311+G(3d) basis sets at sulfur and the 6-311+G(d,p) basis sets at the other atoms. This basis set combination is denoted III+ and was successfully employed for other reactions of third row transition metals.<sup>29</sup> Activation and reaction free energies ( $\Delta G_a$ ,  $\Delta G_r$ ) were calculated by adding corrections from unscaled zero-point energy (ZPE), thermal energy, work, and entropy evaluated at the B3LYP/II- level at 298.15 K, 1 atm to the activation and reaction energies ( $\Delta E_a$ ,  $\Delta E_r$ ), which were calculated at the B3LYP/III+/II- level.

**Solvation Free Energies.** Solvation free energies  $G_{\text{solv}}^\epsilon$  of the structures optimized at the B3LYP/II- level (vide supra) were calculated by Poisson–Boltzmann (PB) calculations with a dielectric constant  $\epsilon$  of the dielectric continuum that represents the solvent. Atomic charges that fit the electrostatic potential of the gas phase wave function were calculated for the numerical solution of the PB equations. To represent the reaction field that is caused by the polarization of the dielectric continuum surrounding the molecule, charges on the molecular surface were generated. These surface charges were in turn used for calculating the molecular wave function, and the iterative procedure was carried out until self-consistency. The PB calculations were performed at the B3LYP level using the LACV3P++\*\* basis set on platinum and the 6-31G\*\* basis set on the other atoms as implemented in the Jaguar 5 program package.<sup>30</sup> The continuum boundary in the PB calculations was defined by a solvent-accessible molecular surface with a set of atomic radii for H (1.150 Å), C (1.900 Å), N (1.600 Å), O (1.600 Å), S (1.900 Å), Cl (1.974 Å), and Pt (1.377 Å) as recommended by Baik et al. (B02)<sup>4b,31</sup> in a recent DFT/CDM study of diamminechloroplatinum(II) derivatives. Test calculations using the slightly different set of atom-type radii reported by Friesner and co-workers (F02)<sup>32</sup> led to a change of +0.5 kcal/mol in the activation free energy for the substitution of the aqua ligand in diammineaquachloroplatinum(II) by 5-methylimidazole and to a change in the activation free energy of –2.8 kcal/mol in the reaction of diamminediaquaplata-nium(II) by 9-methylguanine. In general, I prefer a definition of the molecular cavity based on atoms (such as “carbon”) rather than on atom types (such as “carbon, sp<sup>2</sup>”), because assigning atom types may

be arbitrary along reaction coordinates of chemical reactions that involve changes of atom types. Karplus and co-workers<sup>33</sup> previously employed the powerful Poisson–Boltzmann solver of the Jaguar program to predict relative  $pK_a$ 's of phosphoranes. With the F02 radius of 1.90 Å at sulfur, relative experimental  $pK_a$ 's of aromatic and aliphatic thiols<sup>34</sup> were reproduced with a remarkable accuracy, as demonstrated by a slope A of 1.08 in the linear fitting relation,  $pK_a(\text{fit}) = A pK_a(\text{raw}) + B$ .<sup>32</sup> The axis intercept B of –6.89 indicates the calculated absolute  $pK_a$  values,  $pK_a(\text{raw})$ , to be systematically too high. This result (i) might indicate the uncertainty in the experimental hydration free energy of the H<sup>+</sup> ion,<sup>35</sup> which was used for the calculation of raw  $pK_a$  values via a thermodynamic cycle,<sup>36</sup> or (ii) might suggest the refinement of the definition of the molecular cavity toward a smaller radius at sulfur, which would predict a more negative solvation free energy, particularly of the anionic thiolate and thus lower  $pK_a(\text{raw})$  values. To investigate the latter suggestion, test calculations of the  $pK_a$ 's of thiols have been performed. The  $pK_a$  predictions for methanethiol and benzenethiol were carried out using the thermodynamic cycle<sup>36</sup>

$$\Delta G^\epsilon = \Delta G^1 + G_{\text{solv}}^\epsilon(\text{H}^+) + G_{\text{solv}}^\epsilon(\text{RS}^-) - G_{\text{solv}}^\epsilon(\text{RSH})$$

$$pK_a^\epsilon = -\lg \exp(-\Delta G^\epsilon/R'T) = \Delta G^\epsilon/R'T \ln 10$$

where  $\Delta G^1$  and  $\Delta G^\epsilon$  are the reaction free energies of the reaction,  $\text{RSH} \rightarrow \text{RS}^- + \text{H}^+$ , in vacuo<sup>37</sup> and at  $\epsilon = 80$  for water, respectively,  $G_{\text{solv}}^\epsilon(\text{X})$  is the solvation free energy of species X at  $\epsilon = 80$  obtained via PB calculations,  $R'$  is the ideal gas constant, and  $T$  is the temperature (298.15 K). The calculations demonstrate that the B02 and F02 radius of 1.90 Å at sulfur is the best choice and accurate  $pK_a$  values can be predicted, if an experimental value of –260.9 kcal/mol is used for the hydration free energy of the H<sup>+</sup> ion ( $G_{\text{solv}}^{80}(\text{H}^+)$ ), as recommended by Truhlar and co-workers<sup>35a</sup> (see Supporting Information, Table S-5). Overall, I expect an accuracy of the DFT/CDM approach of ~5 kcal/mol and a significantly higher accuracy of the predicted trends. Test calculations show that the activation free energy for the substitution of the aqua ligand in **1** with methylthiolate changed by +3.5 kcal/mol when a radius of 1.70 Å instead of 1.90 Å was used at sulfur. The energetics of the reactions with thioethers apparently do not significantly depend on the sulfur radius in the PB calculations, as demonstrated by the fact that the activation free energy for the substitution of the aqua ligand in **1** with dimethyl sulfide changed by only +0.03 kcal/mol when a radius of 1.70 Å instead of 1.90 Å was used at sulfur.

The  $pK_a$  of methanethiol in dependence of the dielectric constant was computed using the thermodynamic cycle.<sup>36</sup> The solvation free energies  $G_{\text{solv}}^\epsilon$  of the H<sup>+</sup> ion at various  $\epsilon$  were calculated using the scaling equation

$$G_{\text{solv}}^\epsilon = G_{\text{solv}}^{80} (80/79) (1 - \epsilon^{-1})$$

derived from the Born model.<sup>38</sup> A value of –260.9 kcal/mol has been used again for the hydration free energy of the H<sup>+</sup> ion ( $G_{\text{solv}}^{80}$ ).<sup>35a</sup> The calculations show thiols to be very likely protonated at low  $\epsilon$  (see Supporting Information, Table S-6).

#### Energy Decomposition Analyses along Reaction Coordinates.

Selected structures on the reaction coordinate were analyzed using the

- (25) Frisch, M. J.; Trucks, G. W.; Schlegel, H. B.; Scuseria, G. E.; Robb, M. A.; Cheeseman, J. R.; Zakrzewski, V. G.; Montgomery, J. A., Jr.; Stratmann, R. E.; Burant, J. C.; Dapprich, S.; Millam, J. M.; Daniels, A. D.; Kudin, K. N.; Strain, M. C.; Farkas, O.; Tomasi, J.; Barone, V.; Cossi, M.; Cammi, R.; Mennucci, B.; Pomelli, C.; Adamo, C.; Clifford, S.; Ochterski, J.; Petersson, G. A.; Ayala, P. Y.; Cui, Q.; Morokuma, K.; Malick, D. K.; Rabuck, A. D.; Raghavachari, K.; Foresman, J. B.; Cioslowski, J.; Ortiz, J. V.; Stefanov, B. B.; Liu, G.; Liashenko, A.; Piskorz, P.; Komaromi, I.; Gomperts, R.; Martin, R. L.; Fox, D. J.; Keith, T.; Al-Laham, M. A.; Peng, C. Y.; Nanayakkara, A.; Gonzalez, C.; Challacombe, M.; Gill, P. M. W.; Johnson, B. G.; Chen, W.; Wong, M. W.; Andres, J. L.; Head-Gordon, M.; Replogle, E. S.; Pople, J. A. *Gaussian 98*, revision A.11.1; Gaussian, Inc.: Pittsburgh, PA, 1998.
- (26) Hay, P. J.; Wadt, W. R. *J. Chem. Phys.* **1985**, *82*, 299.
- (27) (a) Binkley, J. S.; Pople, J. A.; Hehre, W. J. *J. Am. Chem. Soc.* **1980**, *102*, 939. (b) Hehre, W. J.; Ditchfield, R.; Pople, J. A. *J. Chem. Phys.* **1972**, *56*, 2257.
- (28) Ehlers, A. W.; Böhme, M.; Dapprich, S.; Gobbi, A.; Höllwarth, A.; Jonas, V.; Köhler, K. F.; Stegmann, R.; Veldkamp, A.; Frenking, G. *Chem. Phys. Lett.* **1993**, *208*, 111.
- (29) (a) Deubel, D. V.; Frenking, G. *J. Am. Chem. Soc.* **1999**, *121*, 2021. (b) Deubel, D. V.; Sundermeyer, J.; Frenking, G. *J. Am. Chem. Soc.* **2000**, *122*, 10101. (c) Deubel, D. V.; Schlecht, S.; Frenking, G. *J. Am. Chem. Soc.* **2001**, *123*, 10085. (d) Deubel, D. V. *Angew. Chem., Int. Ed.* **2003**, *42*, 1974. (e) Deubel, D. V.; Frenking, G. *Acc. Chem. Res.* **2003**, *36*, 645. (f) Deubel, D. V. *J. Am. Chem. Soc.* **2003**, *125*, 15308. (g) Deubel, D. V.; Muñiz, K. *Chem.–Eur. J.* **2004**, *10*, in press. (h) Deubel, D. V. *J. Am. Chem. Soc.* **2004**, *126*, 996.
- (30) *Jaguar 5.0*; Schrödinger, Inc.: Portland, OR, 2000. See: Vacek, G.; Perry, J. K.; Langlois, J.-M. *Chem. Phys. Lett.* **1999**, *310*, 189.
- (31) See, for example: (a) Rashin, A. A.; Honig, B. *J. Phys. Chem.* **1985**, *89*, 5588. (b) Gilbert, T. M.; Hristov, I.; Ziegler, T. *Organometallics* **2001**, *20*, 1183. (c) Cooper, J.; Ziegler, T. *Inorg. Chem.* **2002**, *41*, 6614. (d) Baik, M. H.; Friesner, R. A. *J. Phys. Chem. A* **2002**, *106*, 7407.
- (32) Klicic, J. J.; Friesner, R. A.; Liu, S.-Y.; Guida, W. C. *J. Phys. Chem. A* **2002**, *106*, 1327.

- (33) Lopez, X.; Schaefer, M.; Dejaegere, A.; Karplus, M. *J. Am. Chem. Soc.* **2002**, *124*, 5010.
- (34) Exptl.  $pK_a$ 's: 10.3 (MeSH), 6.6 (PhSH, ref 32), and 8.3 (cysteine, ref 10).
- (35) (a) Chambers, C. C.; Hawkins, G. D.; Cramer, C. J.; Truhlar, D. G. *J. Phys. Chem.* **1996**, *100*, 16385. (b) Tawa, G. J.; Topol, I. A.; Burt, S. K.; Caldwell, R. A.; Rashin, A. A. *J. Chem. Phys.* **1998**, *109*, 4852. (c) Mejias, J. A.; Lago, S. *J. Chem. Phys.* **2000**, *113*, 7306.
- (36) Jorgensen, W. L.; Briggs, J. M.; Gao, J. *J. Am. Chem. Soc.* **1987**, *109*, 6857.
- (37) Not surprisingly, the reaction energy of the reaction,  $\text{CH}_3\text{SH} \rightarrow \text{CH}_3\text{S}^- + \text{H}^+$ , calculated at B3LYP/III+/II- in a vacuum (355.9 kcal/mol) is close to the experimental value (356.9 kcal/mol, ref 32) as well as to the reaction energy calculated at CCSD(T)/III+/B3LYP/II- (358.0 kcal/mol).
- (38) (a) Tomasi, J.; Persico, M. *Chem. Rev.* **1994**, *94*, 2027. (b) Cramer, C. J.; Truhlar, D. G. *Chem. Rev.* **1999**, *99*, 2161.

Ziegler–Rauk energy decomposition scheme<sup>9,39,40</sup> at the BLYP<sup>22,24</sup>/ZORA<sup>41</sup>/IV+ level (using the large TZV2P and TZVP basis set at platinum and the other atoms, respectively)<sup>42</sup> as implemented in the Amsterdam Density Functional 2002 program (ADF). Bickelhaupt et al.<sup>43</sup> reported a strong dependence of the energy components in the Ziegler–Rauk analysis of N–F bonds on the distance between the fragments considered. Note that in particular transition structures are the *result* of the distance dependence and not vice versa. Therefore, a direct comparison of the analysis of the TSs can be misleading, unless they occur at a very similar extent of reaction. Structures with a similar Pt–O(aqua) distance, which is a measure of the extent of reaction in the reactions studied, were generated by adding to the TS geometry a fraction of the Hessian eigenvector that corresponds to the imaginary frequency.<sup>44</sup> The consistent change in the energy components in the TS region given in Figure 1 and Tables S-3 and S-4 demonstrates that few points are sufficient rather than a computationally expensive analysis of the entire intrinsic reaction coordinate. The energy of each structure is decomposed by considering the two reactants (“fragments”), **1** or **2** and NH<sub>3</sub> or SH<sub>2</sub>, interacting with each other. The activation energy is the energy sum of two contributions ( $Sum = Str + Int$ ) at the transition state. The activation free energies are systematically higher than the activation energies due to the loss of translational and rotational entropy in the associative mechanism of the nucleophilic substitution at the metal. Strain energy *Str* is the difference between the energy of the isolated fragments in the geometry of the structure analyzed and the sum of the energy of the two fragments in their equilibrium

geometry. *Int* is the energy of interaction between the fragments and can in turn be partitioned into three components ( $Int = Elst + Pauli + Orb$ ). *Elst* gives the electrostatic interaction energy between the fragments, which is calculated with a frozen electron-density distribution in the TS geometry. Pauli repulsion (*Pauli*) considers the energy required for antisymmetrization and renormalization of the Kohn–Sham orbitals of the superimposing fragments. *Pauli* represents the repulsive interaction energy between the fragments that is caused by the fact that two electrons with the same spin cannot occupy the same region in space (Pauli principle). Finally, the stabilizing orbital interaction term *Orb* is calculated with the Kohn–Sham orbitals relaxing to their optimal form. The Ziegler–Rauk energy decomposition scheme<sup>39</sup> and Dapprich and Frenking’s approach<sup>45</sup> are chemically intuitive and have become very popular, particularly in recent DFT studies of transition-metal complexes.<sup>29</sup>

**Acknowledgment.** The author thanks Justin K. C. Lau for helpful discussions. This work was supported by Michele Parrinello, the Swiss National Science Foundation (Grant 2100-068023.02), the Swiss Center for Scientific Computing, the Fonds der Chemischen Industrie, and the Federal Ministry of Education and Research, Germany.

**Supporting Information Available:** Data tables, drawings, and Cartesian coordinates of calculated structures of TS and products (PDF). This material is available free of charge via the Internet at <http://pubs.acs.org>.

JA0499602

- (39) (a) Morokuma, K. *J. Chem. Phys.* **1971**, *55*, 1236. (b) Ziegler, T.; Rauk, A. *Theor. Chim. Acta* **1977**, *46*, 1.
- (40) (a) Frenking, G.; Fröhlich, N. *Chem. Rev.* **2000**, *100*, 717. (b) Frenking, G.; Wichmann, K.; Fröhlich, N.; Loschen, C.; Lein, M.; Frunzke, J.; Rayón, V. M. *Coord. Chem. Rev.* **2003**, *238*, 55.
- (41) Van Lenthe, E.; Ehlers, A. E.; Baerends, E. J. *J. Chem. Phys.* **1999**, *110*, 8943 and references cited therein.
- (42) This level of theory proved to be successful in former energy decomposition analyses, e.g., Deubel, D. V. *J. Am. Chem. Soc.* **2002**, *124*, 12312.
- (43) Bickelhaupt, F. M.; DeKock, R.; Baerends, E. J. *J. Am. Chem. Soc.* **2002**, *124*, 1500.

- (44) The following fractions of the eigenvector were added to the TS coordinates to match the Pt–O(aqua) distance: **1** + NH<sub>3</sub>: –31% (2.36 Å), 0% (2.42 Å, TS), 31% (2.48 Å). **1** + H<sub>2</sub>S: 42% (2.36 Å), 21% (2.42 Å), 0% (2.48 Å, TS). **2** + NH<sub>3</sub>: –12% (2.36 Å), 0% (2.387 Å, TS, not analyzed), 16% (2.42 Å), 44% (2.48 Å). **2** + H<sub>2</sub>S: –54% (2.36 Å), –27% (2.42 Å), 0% (TS, 2.48 Å, TS).
- (45) Dapprich, S.; Frenking, G. *J. Phys. Chem.* **1995**, *99*, 9352.